Research Letter **DOI:** 10.15541/jim20240085

Effect of Elastic Strains on Adsorption Energies of C, H and O on Transition Metal Oxides

XIE Tian[1], SONG Erhong[2]

(1. School of Materials Science and Engineering, Shanghai Jiao Tong University, Shanghai 200240, China; 2. Shanghai Institute of Ceramics, Chinese Academy of Sciences, Shanghai 200050, China)

Abstract: Platinum (Pt)-based noble metal catalysts (PGMs) are the most widely used commercial catalysts, but they have the problems of high cost, low reserves, and susceptibility to small-molecule toxicity. Transition metal oxides (TMOs) are regarded as potential substitutes for PGMs because of their stability in oxidizing environments and excellent catalytic performance. In this study, comprehensive investigation into the influence of elastic strains on the adsorption energies of carbon (C), hydrogen (H) and oxygen (O) on TMOs was conducted. Based on density functional theory (DFT) calculations, these effects in both tetragonal structures (PtO_2, PdO_2) and hexagonal structures (ZnO, CdO), along with their respective transition metals were systematically explored. It was identified that the optimal adsorption sites on metal oxides pinpointed the top of oxygen or the top of metal atom, while face-centered cubic (FCC) and hexagonal close-packed (HCP) holes were preferred for the transition metals. Furthermore, under the influence of elastic strains, the results demonstrated significant disparities in the adsorption energies of H and O between oxides and transition metals. Despite these differences, the effect of elastic strains on the adsorption energies of C, H and O on TMOs mirrored those on transition metals: adsorption energies increased under compressive strains, indicating weaker adsorption, and decreased under tension strains, indicating stronger adsorption. This behavior was rationalized based on the d-band model for adsorption atop a metallic atom or the p-band model for adsorption atop an oxygen atom. Consequently, elastic strains present a promising avenue for tailoring the catalytic properties of TMOs.

Key words: density functional theory; adsorption energy; elastic strain engineering; transition metal oxide; catalyst

Platinum (Pt)-based metallic materials are widely recognized as benchmark catalysts for pivotal electrochemical reactions such as the hydrogen evolution reaction (HER) and the oxygen reduction reaction (ORR), which are pivotal processes governing hydrogen generation from water and energy production in fuel cells[1]. Similarly, catalysts based on precious metals-based materials exhibit superior electrocatalytic performance for essential reactions like the CO_2 reduction reaction (CO_2RR) and nitrogen reduction reaction (NRR) among diverse applications, which is crucial for carbon capture and ammonia production[2-4]. However, the substantial cost and limited availability of these precious metals underscore the imperative to explore cost-effective alternatives with comparable catalytic activity and long-term stability in demanding catalytic environments.

Transition metals oxides (TMOs) hold promise for stability in oxidizing environments. For instance, RuO_2 and IrO_2 are renowned catalysts for the oxygen evolution reaction (OER)[5-7]. Moreover, TMOs based on metals like Co, Mn, Fe, or Ni[8-11] have long been considered as promising electrocatalysts[12], given their favorable cost-effectiveness ratio and robust stability during electrocatalytic process. The intricate electronic structure of TMOs offers avenues to fine-tune their catalytic performance[13-14]. Strategies to enhance the catalytic efficiency and stability of TMOs in electrocatalysis include nanostructured synthesis[15], vacancy engineering[16-17],

Received date: 2024-02-28; **Revised date:** 2024-06-12; **Published online:** 2024-06-24
Foundation item: Science and Technology Commission of Shanghai Municipality (21ZR1472900, 22ZR1471600)
Biography: XIE Tian (1993–), male, PhD. E-mail: xietian1993@sjtu.edu.cn
谢 天(1993–), 男, 博士. E-mail: xietian1993@sjtu.edu.cn
Corresponding author: SONG Erhong, associate professor. E-mail: ehsong@mail.sic.ac.cn
宋二红, 副研究员. E-mail: ehsong@mail.sic.ac.cn

doping[18-19] and the interactions with metallic substrates.

Elastic strain engineering emerges as another promising strategy to augment surface catalytic performance. Substantial elastic deformations modify interatomic distances and electronic structures, thereby influencing physical and chemical properties. Recent recognition on this approach's potential to modulate the catalytic properties of multi-metallic materials[20-21] highlights its significance. Mechanical strains have been identified as key contributors to the enhanced catalytic properties of Pt-based nanoparticles for the HER[22] and the ORR[23]. However, investigations into the impact of elastic strains on TMO catalytic properties remain scarce. While Amakawa *et al*.[24] explored how strain affects the reactivity of surface metal oxide catalysts, and they proposed that elastic strains should be an additional descriptor of the catalytic processes involving supported metal oxides. Ling *et al*.[25] demonstrated that applying tensile strains to CoO nanorods enhances the HER performance by generating oxygen vacancies. However, a systematic study on the influence of elastic strains on TMO adsorption energies remains unexplored.

Catalytic performance is mediated by molecule and atom adsorption on catalyst surface, assessable through density functional theory (DFT) calculations. Pioneered work by Nørskov *et al*.[26] utilized DFT to calculate adsorption free energies on various surfaces, replicating experimental volcano plots for the HER. This methodology has been extensively employed to screen catalysts and elucidate catalytic process intricacies for diverse reactions. Martínez-Alonso *et al*.[27-28] applied DFT to explore the effect of elastic strains on the catalytic activity for the HER and the ORR in transition metals (TMs).

This work systematically explored, using DFT calculations, the effect of elastic strains on the adsorption energies of three key adsorbates (H, O, and C) on four distinct TMOs (ZnO, CdO, PdO_2, and PtO_2). Additionally, this investigation was extended to corresponding TMs (Zn, Cd, Pd, and Pt) to discern differences and similitudes between TM and TMO. This inquiry represents an initial step towards leveraging elastic strain engineering to optimize the catalytic properties of TMOs.

1　Computational methods

Four TMOs were selected to explore the influence of elastic strains on the adsorption energies of H, O and C. Two of them were ZnO and CdO that have hexagonal structures, and representative of MO-type oxides in which the most stable surface is (0001). The other two were PdO_2 and PtO_2 that share the same tetragonal structure with (110) as the most stable surface. They are representative of MO_2-type oxides. In addition, the effect of elastic strains was also determined on the (0001) surfaces of Zn and Cd, which have a hexagonal close-packed lattice, and on the (111) surfaces of Pd and Pt, which have a face-centered cubic lattice.

The adsorption energies of H, O and C on each location of the slab surface could be obtained as follows:

$$E_{\mathrm{ads}}^{\mathrm{H}} = E_{\mathrm{slab+H}} - E_{\mathrm{slab}} - \frac{1}{2}E_{\mathrm{H_2}} \tag{1}$$

$$E_{\mathrm{ads}}^{\mathrm{O}} = E_{\mathrm{slab+O}} - E_{\mathrm{slab}} - \frac{1}{2}E_{\mathrm{O_2}} \tag{2}$$

$$E_{\mathrm{ads}}^{\mathrm{C}} = E_{\mathrm{slab+C}} - E_{\mathrm{slab}} - E_{\mathrm{C}} \tag{3}$$

where E_{slab} is the energy for the clean slab, and $E_{\mathrm{slab+H}}$, $E_{\mathrm{slab+O}}$, and $E_{\mathrm{slab+C}}$ stand for energies of each slab with adsorbates. $E_{\mathrm{H_2}}$, $E_{\mathrm{O_2}}$ and E_{C} account for the total energies of the isolated hydrogen, oxygen molecule, and carbon atom.

All of these quantitates were calculated by DFT simulations on (2×2) slabs of either TM or TMO with four layers of atoms perpendicular to the surface. The slabs were generated using the atomic simulation environment (ASE)[29] from the equilibrium lattice parameters of the bulk structures that were obtained from the materials project website[30] after relaxation. The periodic slabs were separated by 15 Å of vacuum in the direction perpendicular to the surface to avoid interactions due to the periodic boundary conditions (Fig. 1). Adsorption energies of chemical species were calculated assuming coverage of 1/4 monolayers. All metal atoms in the top two layers of the slab and all adsorbed H, O, and C were fully relaxed, while the positions of atoms in the bottom two layers were fixed using the lattice values of

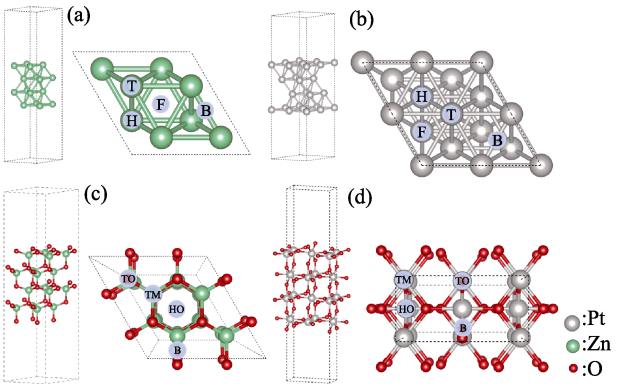

Fig. 1　Lateral and top views of (2×2×4) slab models
(a) (0001) surface of hexagonal close-packed Zn; (b) (111) surface of face-centered cubic Pt; (c) (0001) surface of hexagonal ZnO; (d) (110) surface of tetragonal PtO_2; Surfaces are separated by 15 Å of vacuum; T, B, H, and F stand for top, bridge, HCP hollow, and FCC hollow adsorption sites in (a, b); TO, TM, HO, and B stand for top of O, top of metal, hollow, and metal-oxygen bridge adsorption sites in (c, d)
Colorful figures are available on website

the bulk. The slab of the (0001) Zn surface is depicted in Fig. 1(a), while that of (111) Pt can be found in Fig. 1(b). They are also representatives of hexagonal close-packed Cd and the face-centered cubic Pd, respectively. Similarly, the slabs of (0001) ZnO and of (110) PtO_2 are plotted in Fig. 1(c, d), respectively, and also stand for tetragonal CdO and hexagonal PdO_2. More details of the adsorption structure can be found in Fig. S1 for Cd, CdO and Pd, PdO_2, which are structurally similar to Zn, ZnO and Pt, PtO_2, respectively. The most stable adsorption cases can be obtained in detail from Table 1.

The surfaces in Fig. 1 were subjected to biaxial stresses in the surface plane. Mixed boundary conditions were imposed to solve the elastic problem in the DFT calculations. They include imposed strains in the slab plane and zero stresses on the free surface. The applied deformation gradient F was

$$F = \begin{pmatrix} 1+\varepsilon & 0 & 0 \\ 0 & 1+\varepsilon & 0 \\ 0 & 0 & 1 \end{pmatrix} \quad (4)$$

where ε is the magnitude of the biaxial strain in the surface plane.

DFT calculations were carried out with the quantum espresso package[31]. The electron exchange correlation was described with the generalized gradient approximation (GGA) of Perdew-Burke-Ernzerhof (PBE)[32], and ultrasoft pseudopotentials. The cut-off energies for the plane waves was set at 80 Ry, and the slab models of the Monkhorst-Pack *k*-points were sized (4×4×4) for TM, (4×4×1) for MO-type TMO, and (8×4×1) for MO_2-type TMO. The charge transfer was calculated using Bader charge analyses[33-35].

2 Results and discussions

2.1 Adsorption energies of H, O, and C on TM and TMO

The adsorption energies of three different adsorbates on the TM and TMO were firstly calculated without the application of elastic strains in the different locations indicated in Fig. 2. Only the adsorption sites with most favorable minimum adsorption energy are depicted in Table 1. The corresponding adsorption energies for all sites can be found in the supplementary information (Table S1 and Table S2). The most favorable adsorption sites for the TM were the HCP and FCC holes for all adsorbates, in agreement with previous experimental and theoretical studies[28]. The adsorption energies decreased along H, O, and C, and the processes were exothermic with the exceptions of the adsorption of H on Zn and Cd.

The most favorable adsorption sites for hexagonal ZnO and CdO TMOs were on top of the oxygen atoms for three adsorbates. On the contrary, O and C were preferentially adsorbed on top of the metallic atoms in tetragonal MO_2 oxides, whereas H was adsorbed on top of the oxygen atoms. Furthermore, the adsorption energies were negative in all cases, indicating exothermic processes except for O on CdO which was slightly endothermic. The minimum adsorption energies were found for C in all cases, which suggests that C had the strongest adsorption interaction with the surfaces of these materials. It should also be noted that the adsorption energy of H on the metal slab was much higher than that on the corresponding oxide slab, and the opposite behavior was found for the adsorption of O.

It is interesting to further analyze the adsorption of O onto ZnO and CdO. Here the adsorption occurs on top of the O atom instead of on top of the metal. In order to better understand this behavior, the Bader atomic charges were calculated for these systems, and the main results are summarized in Table S3. It was found that the metal atoms in PdO_2 and PtO_2 (1.62 and 1.81 a.u.) are charged more positively than those in ZnO and CdO (1.26 and 1.15 a.u.), and this difference explains the reason why O is adsorbed preferentially on top of the metal in the case of PdO_2 and PtO_2 but not ZnO and CdO.

Another interesting feature of the adsorption of O onto ZnO and CdO is that it is less energetically favorable than the adsorption of H. However, the atomic charges associated with both processes (adsorption of O and H) are similar. The electron densities of adsorbed O and H atoms are depleted of 0.02 and 0.43 a.u. in the case of ZnO, while the adsorbed O atom is able to gain

Table 1 Adsorption energies and preferred adsorption sites for H, O, and C on TM and TMO

	Zn	Cd	Pd	Pt	ZnO	CdO	PdO_2	PtO_2
E_{ads}^{H} / eV	0.63	0.81	–0.57	–0.49	–1.94	–0.69	–2.13	–1.05
Adsorption site (H)	HCP	FCC	FCC	FCC	O top	O top	O top	O top
E_{ads}^{O} / eV	–2.41	–2.24	–2.11	–2.16	–0.25	1.17	–0.43	–0.72
Adsorption site (O)	HCP	FCC	FCC	FCC	O top	O top	M top	M top
E_{ads}^{C} / eV	–5.04	–4.70	–7.97	–8.39	–8.32	–4.62	–9.86	–5.43
Adsorption site (C)	FCC	FCC	HCP	FCC	O top	O top	M top	M top

HCP and FCC: adsorption on the corresponding holes of TM lattice; M top and O top: adsorption on top of metal and oxygen atoms (Fig. 1)

electronic density (–0.41 a.u.) and the adsorbed H atom only loses 0.07 a.u. in CdO. These small differences in charge transfer suggest that the physical phenomena that control adsorption are similar in both cases.

2.2 Effect of elastic strains on adsorption energies of H, O, and C

Biaxial elastic strains ranging from –5% to 5% were applied to the surface slabs and the corresponding adsorption energies were calculated using Eq. (1–3) for each adsorbate. In some cases, the slabs were destroyed by the applied biaxial strain because it went beyond the mechanical stability limit of the slabs, and it was not possible to determine the corresponding adsorption energy. For instance, this occurred when C was adsorbed on ZnO under 3% of compressive biaxial strain. C atom moved into the second layer of the metallic slab, leading to fracture. Mechanical instabilities generally occur at lower strains under compression compared to tension. Additionally, hexagonal transition metals like Zn and Cd, and their corresponding oxides ZnO and CdO, exhibit these instabilities at even lower compressive strains. Hexagonal metals (Cd, Zn) attained the mechanical instability limits at lower strains than the corresponding TMO (CdO, ZnO).

The influence of elastic strains on the adsorption energies of H, O, and C on TM and TMO is depicted in Fig. S2. Tensile strains reduced the adsorption energy in TM while compressive strains led to the opposite behavior, in agreement with previous data[28, 36], while TMO followed the same behavior. More quantitative information of the actual influence of the elastic strains on the adsorption energies is given by $E^{X}_{ads}(\varepsilon)-E^{X}_{ads}(0)$. This parameter for H, O and C adsorbed onto hexagonal TM and TMO is plotted in Fig. 2(a–c), respectively, while for H, O, and C adsorbed onto cubic TM and tetragonal TMO is plotted in Fig. 2(d–f). Cubic TM and tetragonal TMO (MO_2) were able to sustain larger elastic strains without fracture, and the effect of elastic strains on the adsorption energy could be explored in the whole range from –5% to 5% for the majority of the adsorbates and surfaces in Fig. 2(d–f). The influence of elastic strains on the MO_2 oxides was qualitatively similar to that found in the corresponding TM. In general, adsorption on Pt is more sensitive to strains than that on PtO_2, while the strain sensitivities on the adsorption of C and H are similar in the cases of Pd and PdO_2. Mechanical instabilities developed in the case of hexagonal TM and TMO subjected to biaxial strains, and the effect of elastic strains on both systems could not be fully explored because of the lack of data for equal strains for both TM and TMO in the whole strain range. Nevertheless, the overall trend observed for MO_2 seems to hold for MO oxides.

2.3 Electronic structure

The effect of elastic strains on adsorption energy of TM has been rationalized by the so-called d-band model[37-38]. Basically, this model establishes that the variation in the adsorption energy from one TM surface to another correlates with the upward shift of d-band center ϵ_d with respect to the Fermi level. A shift towards higher energies allows the formation of a larger number of empty anti-bonding states, leading to stronger (more negative) binding energy. Tensile strains shift the ϵ_d towards higher energies for TM, leading to more

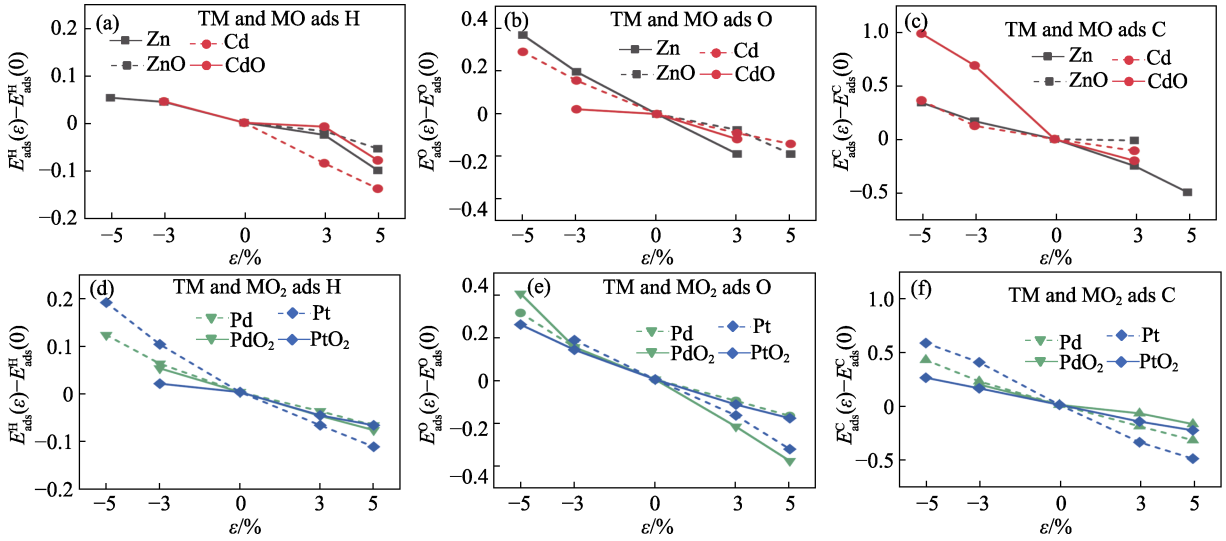

Fig. 2　Variation of the adsorption energy under biaxial strain with respect to the unstrained state $E^{X}_{ads}(\varepsilon)-E^{X}_{ads}(0)$ for different absorbates as a function of the biaxial strain ε

Hexagonal Zn and Cd as well as ZnO and CdO, adsorbed with (a) H, (b) O, and (c) C;
Cubic Pd and Pt as well as tetragonal PdO_2 and PtO_2, adsorbed with (d) H, (e) O and (f) C

favorable adsorption energies, while compressive (and shear strains) produces a shift towards lower d-band center and leads to less favorable interactions[39-40]. The validity of the d-band model was thoroughly evaluated in eleven TM in which the adsorption energies of H, O and OH were determined as a function tensile, compressive and shear strains[28]. It was found that the overlap of metal d-states at neighboring sites either increases or decreases when the surface undergoes compressive or tensile strains, and so do the d-band widths in order to maintain constant filling. Thus, compressive strain leads to a downshift of the d-band centers, while tensile strain leads to an upshift[41]. Moreover, compared with the effect of strains, the adsorption of either H, O or C led to small changes on the projected density of the states (PDOS) on the d-band onto the surface of all metals, and a linear relationship between the adsorption energy and the Fermi energy level of each clean, strained surface was established for each adsorbate.

Following these results, the adsorption energy is plotted in Fig. 3 as a function of the Fermi energy of the strained slab in which the adsorbate (H, O or C) has been adsorbed on the TM and TMO. Following the d-band model, there is a linear relationship between adsorption energy and the Fermi energy for each adsorbate and TM (Fig. 3(a–c)). Both increase with compressive strains and decrease under tensile strains. Results for the hexagonal (MO) and tetragonal (MO_2) TMO follow the same trend (Fig. 3(d–f)), in agreement with the overall influence of elastic strains on the adsorption energy in TMO: tensile strains favor adsorption, while compressive strains favor desorption, and the relationship between the adsorption energy and the Fermi level is linear.

In order to understand the effect of elastic strains on the adsorption energy of TMO, the PDOS onto 5d orbitals of the Pt atom nearest to the adsorbate with C and O adsorbed, and onto 2p orbitals of the O atom nearest to the adsorbate with H adsorbed on the (111) PtO_2 surface were calculated. The PDOS onto 5d orbitals of Pt atom in the clean slab and in the slab with C and O adsorbed under the unstrained condition are plotted in Fig. 4(a), together with the PDOS onto 2p orbitals of the O atom in the clean slab and in the slab with H adsorbed in the unstrained condition (dashed lines). The shape and position of the peaks change towards lower energies with H adsorbed onto the surface of PtO_2, while the adsorption of C or O leads to greater changes in the PDOS. H atom is small and possesses a simple electronic structure, leading to limited interactions with the electronic structure of PtO_2. On the contrary, the addition of C changes completely the shape of the bands. Two regions appear, one above 0 and the other with a shoulder on the left of the original PDOS. Finally, the O adsorption produces the same changes as the C adsorption, but slightly shifted to the left.

The evolution of the PDOS following the change of elastic strains on the clean slab is plotted in Fig. 4(b). Elastic deformations do not change the shape of the PDOS but the peaks move towards higher (lower) energies under tensile (compressive) strains, in agreement with the behavior of TM[28]. The effect of strains on the

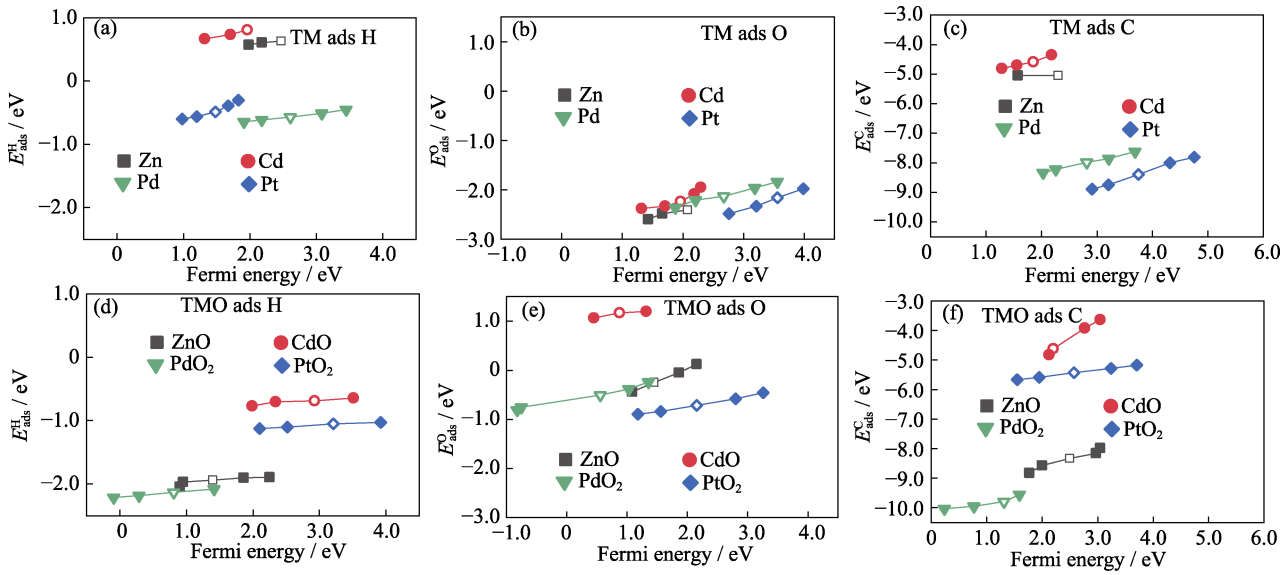

Fig. 3 Adsorption energies of strained slabs as a function of the Fermi energy in the strained slab with the corresponding adsorbate

(a) H, (b) O and (c) C adsorption on TM; (d) H, (e) O and (f) C adsorption on TMO

Empty symbol: adsorption energy without strain; Solid symbol on the left of empty symbol: adsorption energy under biaxial tensile strains; Solid symbol on the right of empty symbol: adsorption energy under biaxial compressive strains

PDOS of the slabs with H, O and C atoms adsorbed is plotted in Fig. 4(c–e), respectively, and follows the same trend observed in the clean slab: the peaks move towards higher energy under tensile strain, and towards lower energy under compressive strain. The positions of the p-band center for H adsorbate and the d-band centers for O and C adsorbates, subjected to different biaxial strains as well as for the clean slab are plotted in Fig. 4(f). Compressive strains move the p-band center of the O atom and d-band center of the Pt atom towards lower energies, leading to higher adsorption energies and lower stability, and on the contrary in the case of tensile strains. Thus, the effect of elastic strains on the adsorption energies of H, O and C on tetragonal TMOs follows the same pattern as that in the case of the corresponding TMs. Therefore, the displacement of the d-band, and p-band of the oxygen in the case of H adsorption center is able to explain the influence of elastic strains on the adsorption energy in TMOs and TMs.

In the case of hexagonal MO-type oxides, the preferred adsorption site of H, O and C was always on top of O atom. Thus, it was assumed that the p-band center instead of the d-band center could be a good descriptor of the adsorption energy[42]. The PDOS onto 2p orbital of O atom in which adsorption took place on the (110) ZnO surface were calculated for different adsorbates and applied strains (Fig. 5). The PDOS of the clean, unstrained slab and the slab with H, O and C adsorbed are depicted in Fig. 5(a). Adsorption of H leads to negligible changes in the PDOS but adsorptions of O and C lead to great shifts of the peaks that can be associated with the favourable adsorption of C (Table 1). The shape of the PDOS changes significantly upon O adsorption due to the formation of O–O interaction and the associated charge depletion, which involves the p-orbitals of both oxygen atoms. Similarly, the PDOS also changes significantly with C adsorption due to the formation of the C–O bond. The C–O contact is 1.16 Å, particularly close, which is comparable to the C–O distance in carbon monoxide and other short C–O interactions[43]. These bonding situations are reflected in the distinctive PDOS features. Application of elastic strains leads to a shift in the peaks of the PDOS of the p orbitals (Fig. 5(b)) that is equivalent to the one in the d orbitals (Fig. 4(b)), but the shapes of the curves are not significantly changed.

The effect of strains on the PDOS of the slabs with H, O and C atoms adsorbed is plotted in Fig. 5(c–e) following the same trend reported for the clean slab (Fig. 5(b)). The position of the p-band center is plotted in Fig. 5(f) for the surfaces with H, O and C adsorbates subjected to different biaxial strains as well as for the clean slab. Compressive strains move the p-band center of the O atom towards lower energies, leading to higher adsorption energies and lower stability, and on the contrary in the case of tensile strains. Thus, based on the

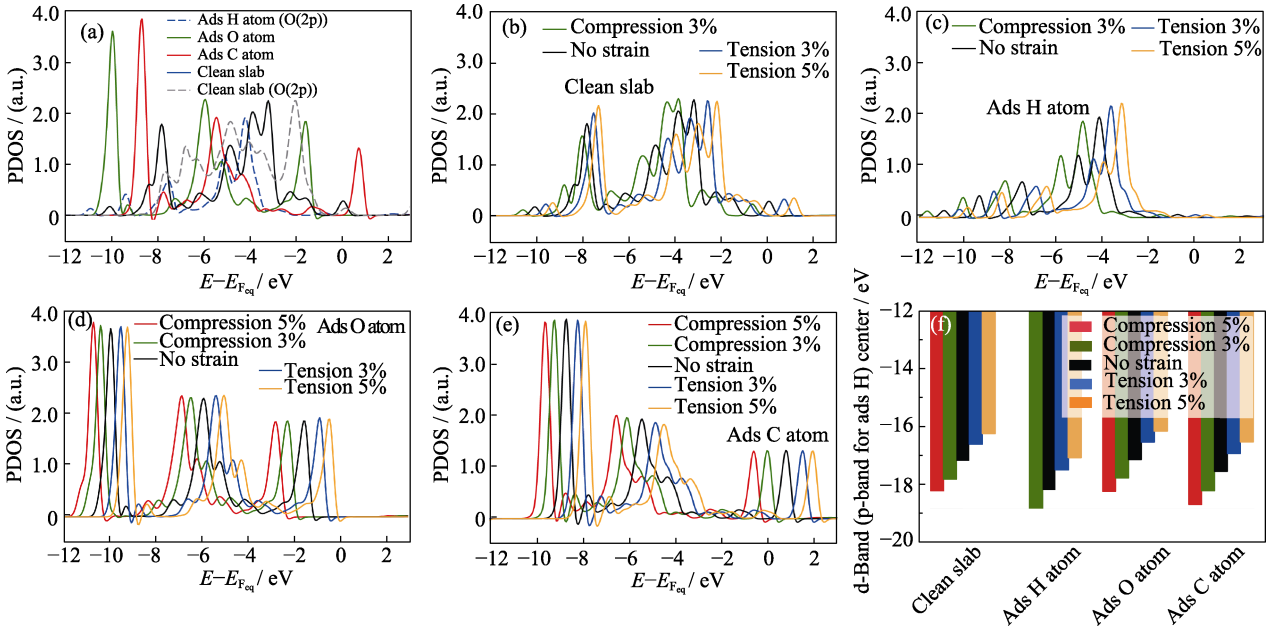

Fig. 4　PDOS onto d orbital of the Pt atom nearest to the C or O adsorbate and PDOS onto p orbital of the O atom nearest to the H adsorbate on the (111) PtO_2 surface

(a) Unstrained, clean slab and unstrained slab with different adsorbates; (b) Clean slab subjected to different biaxial strains; Slabs with (c) H, (d) O, and (e) C adsorbed and subjected to different biaxial strains; (f) Positions of the d-band center of Pt atom close to the C or O adsorbate and of the p-band center of O atom nearest to the H adsorbate on the (111) PtO_2 surfaces subjected to different strains; Energy values are referenced to the Fermi level of the slab; Colorful figures are available on website

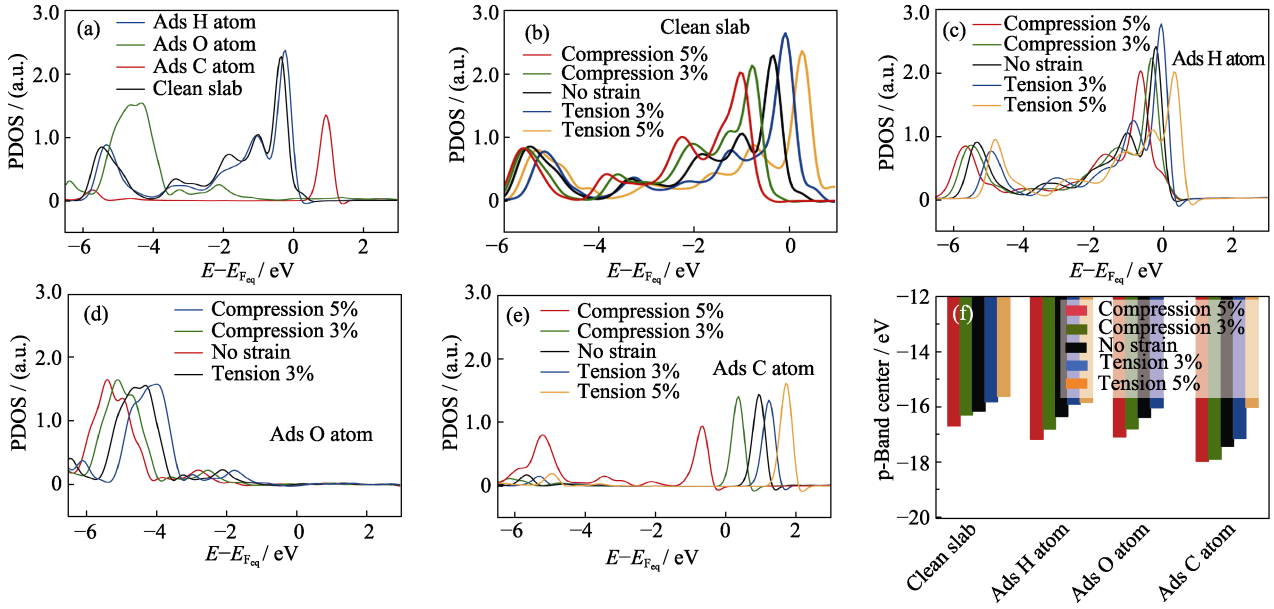

Fig. 5 PDOS onto p orbital of the O atom nearest to the H adsorbate on the (110) ZnO surface

(a) Unstrained, clean slab and unstrained slab with different adsorbates; (b) Clean slab subjected to different biaxial strains; Slabs with (c) H, (d) O, and (e) C adsorbed and subjected to different biaxial strains; (f) Positions of the p-band of O atom nearest to the adsorbate on the (110) ZnO surfaces subjected to different strains; Energy values are referenced to the Fermi level of the slab; Colorful figures are available on website

p-band model, it can be concluded that the effect of elastic strains on the adsorption energies of H, O and C on tetragonal MO-type TMO is equivalent to those on the corresponding TM.

3 Conclusions

DFT calculations revealed how elastic strains influence the adsorption behavior of C, H and O on both transition metal surfaces (Zn, Cd, Pd, and Pt) and their corresponding oxides (ZnO, CdO, PdO_2, and PtO_2). FCC or HCP voids were identified as optimal adsorption sites for C, H, and O on transition metals, with minimal energy discrepancies. Conversely, on metal oxides, H predominantly was adsorbed atop O, while C and O favored adsorption on the metallic atom in tetragonal oxides (PtO_2, PdO_2) and atop O in hexagonal oxides (ZnO, CdO). Notably, H exhibited higher adsorption energy on metal surfaces compared to oxides, whereas O showed the opposite trend. Despite variations in adsorption sites and energies, elastic strains consistently weakened adsorption under compression and strengthened it under tension, aligning with behavior observed for transition metals. This phenomenon was rationalized using the d-band model for adsorption on metallic atom or the p-band model for adsorption on O atom.

The findings underscore the potential of elastic strain engineering as a novel and promising strategy to enhance the catalytic efficiency and stability of TMOs in various electrochemical reactions. This approach opens new avenues for the development of cost-effective, high-performance catalysts that could serve as alternatives to precious metal-based materials. Given the critical role of adsorption processes in catalytic reactions, this research contributes to the fundamental understanding required to tailor TMOs for specific catalytic applications, potentially leading to advancements in green hydrogen production, carbon capture, and other sustainable technologies.

Acknowledgments

The authors would like to acknowledge Prof. Javier Llorca for helpful discussions on DFT calculations. And the computing resources support from the Centro de Supercomputación Visualización de Madrid (CeSViMa), and the computer resources at CTE-Power, and Minotauro in the Barcelona Supercomputing Center, and the computational resources from Shanghai Jiao Tong University Supercomputer Center. This work was also supported by the Center of Hydrogen Science of Shanghai Jiao Tong University.

Supporting materials

Supporting materials related to this article can be found at https://doi.org/10.15541/jim20240085.

References:

[1] KWEON D H, JEON I Y, BAEK J B. Electrochemical catalysts for

green hydrogen energy. *Advanced Energy and Sustainability Research*, 2021, **2(7):** 2100019.

[2] GUO J, JIAO S, YA X, *et al.* Ultrathin Pd‐based perforated nanosheets for fuel cells electrocatalysis. *ChemElectroChem*, 2022, **9(21):** e202200729.

[3] WIJAYA D T, LEE C W. Metal-organic framework catalysts: a versatile platform for bioinspired electrochemical conversion of carbon dioxide. *Chemical Engineering Journal*, 2022, **446(3):** 138311.

[4] XU H, MA Y, CHEN J, *et al.* Electrocatalytic reduction of nitrate-a step towards a sustainable nitrogen cycle. *Chemical Society Reviews*, 2022, **51:** 2710.

[5] FRYDENDAL R, PAOLI E A, KNUDSEN B P, *et al.* Benchmarking the stability of oxygen evolution reaction catalysts: the importance of monitoring mass losses. *ChemElectroChem*, 2014, **1(12):** 2075.

[6] LEE Y, SUNTIVICH J, MAY K J, *et al.* Synthesis and activities of rutile IrO_2 and RuO_2 nanoparticles for oxygen evolution in acid and alkaline solutions. *Journal of Physical Chemistry Letters*, 2012, **3(3):** 399.

[7] WU T, HAN M, ZHU X, *et al.* The electrochemical corrosion of an air thermally-treated carbon fiber cloth electrocatalyst with outstanding oxygen evolution activity under alkaline conditions. *Chemical Communications*, 2019, **55(15):** 2344.

[8] SUEN N T, HUNG S F, QUAN Q, *et al.* Electrocatalysis for the oxygen evolution reaction: recent development and future perspectives. *Chemical Society Reviews*, 2017, **46(2):** 337.

[9] NIE Y, LI L, WEI Z, Recent advancements in Pt and Pt-free catalysts for oxygen reduction reaction. *Chemical Society Reviews*, 2015, **44(8):** 2168.

[10] KULKARNI A, SIAHROSTAMI S, PATEL A, *et al.* Understanding catalytic activity trends in the oxygen reduction reaction. *Chemical Reviews*, 2018, **118(5):** 2302.

[11] DOYLE R L, GODWIN I J, BRANDON M P, *et al.* Redox and electrochemical water splitting catalytic properties of hydrated metal oxide modified electrodes. *Physical Chemistry Chemical Physics*, 2013, **15(33):** 13737.

[12] LANG R, DU X, HUANG Y, *et al.* Single-atom catalysts based on the metal-oxide interaction. *Chemical Reviews*, 2020, **120(21):** 11986.

[13] SUN Y, CHEN G, XI S, *et al.* Catalytically influential features in transition metal oxides. *ACS Catalysis*, 2021, **11(22):** 13947.

[14] KUHLENBECK H, SHAIKHUTDINOV S, FREUND H J. Well-ordered transition metal oxide layers in model catalysis — a series of case studies. *Chemical Reviews*, 2013, **113(6):** 3986.

[15] XIONG W, YIN H, WU T, *et al.* Challenges and opportunities of transition metal oxides as electrocatalysts. *Chemistry*, 2023, **29(5):** e202202872.

[16] XU L, WANG Z, WANG J, *et al.* N-doped nanoporous Co_3O_4 nanosheets with oxygen vacancies as oxygen evolving electrocatalysts. *Nanotechnology*, 2017, **28(16):** 165402.

[17] MOCK S A, SHARP S E, STONER T R, *et al.* CeO_2 nanorods-supported transition metal catalysts for co oxidation. *Journal of Colloid and Interface Science*, 2016, **466:** 261.

[18] MEFFORD J T, RONG X, ABAKUMOV A M, *et al.* Water electrolysis on $La_{1-x}Sr_xCoO_{3-\delta}$ perovskite electrocatalysts. *Nature Communication*, 2016, **7:** 11053.

[19] KUANG X, KANG B, WANG Z, *et al.* Sulfur-doped CoO nanoflakes with loosely packed structure realizing enhanced oxygen evolution reaction. *Chemistry*, 2018, **24(65):** 17288.

[20] LUO M, GUO S. Strain-controlled electrocatalysis on multimetallic nanomaterials. *Nature Reviews Materials*, 2017, **2(11):** 17059.

[21] KHORSHIDI A, VIOLET J, HASHEMI J, *et al.* How strain can break the scaling relations of catalysis. *Nature Catalysis*, 2018, **1(4):** 263.

[22] JIAO Y, ZHENG Y, JARONIEC M, *et al.* Design of electrocatalysts for oxygen- and hydrogen-involving energy conversion reactions. *Chemical Society Reviews*, 2015, **44(8):** 2060.

[23] ESCUDERO-ESCRIBANO, MALACRIDA M P, HANSEN M H, *et al.* Tuning the activity of Pt alloy electrocatalysts by means of the lanthanide contraction. *Science*, 2016, **352(6281):** 73.

[24] AMAKAWA K, SUN L, GUO C, *et al.* How strain affects the reactivity of surface metal oxide catalysts. *Angewandte Chemie International Edition*, 2013, **52(51):** 13553.

[25] LING T, YAN D Y, WANG H, *et al.* Activating cobalt(II) oxide nanorods for efficient electrocatalysis by strain engineering. *Nature Communication*, 2017, **8:** 1509.

[26] NØRSKOV J K, BLIGAARD T, LOGADOTTIR A, *et al.* Trends in the exchange current for hydrogen evolution. *Journal of the Electrochemical Society*, 2005, **152(3):** J23.

[27] MARTÍNEZ-ALONSO C, GUEVARA-VELA J M, JAVIER L L. Understanding the effect of mechanical strains on the catalytic activity of transition metals. *Physical Chemistry Chemical Physics*, 2022, **24(8):** 4832.

[28] MARTÍNEZ-ALONSO C, GUEVARA-VELA J M, JAVIER L L. The effect of elastic strains on the adsorption energy of H, O, and OH in transition metals. *Physical Chemistry Chemical Physics*, 2021, **23(37):** 21295.

[29] BAHN S R, JACOBS K W. An object-oriented scripting interface to a legacy electronic structure code. *Computing in Science & Engineering*, 2002, **4(3):** 56.

[30] JAIN A, ONG S P, HAUTIER G, *et al.* Commentary: the materials project: a materials genome approach to accelerating materials innovation. *APL Materials*, 2013, **1(1):** 011002.

[31] GIANNOZZI P, BARONI S, BONINI N, *et al.* Quantum espresso: a modular and open-source software project for quantum simulations of materials. *Journal of Physics: Condensed Matter*, 2009, **21(39):** 395502.

[32] PERDEW J P, BURKE K, ERNZERHOF M. Generalized gradient approximation made simple. *Physical Review Letters*, 1996, **50(24):** 308.

[33] TANG W, SANVILLE E, HENKELMAN G. A grid-based Bader analysis algorithm without lattice bias. *Journal of Physics: Condensed Matter*, 2009, **21(8):** 084204.

[34] SANVILLE E, KENNY S D, SMITH R, *et al.* Improved grid-based algorithm for Bader charge allocation. *Journal of Computational Chemistry*, 2007, **28(5):** 899.

[35] HENKELMAN G, ARNALDSSON A, JÓNSSON H. A fast and robust algorithm for Bader decomposition of charge density. *Computational Materials Science*, 2006, **36(3):** 354.

[36] HAN J, SUN H, SHI T, *et al.* Rationalization of nonlinear adsorption energy-strain relations and Bronsted-Evans-Polanyi and transition state scaling relationships under strain. *Journal of Physical Chemistry Letters*, 2021, **12(47):** 11578.

[37] HAMMER B N, NØRSKOV J K. Electronic factors determining the reactivity of metal surfaces. *Surface Science*, 1995, **343:** 211.

[38] HAMMER B N, NØRSKOV J K. Why gold is the noblest of all the metals. *Nature*, 1995, **376(20):** 238.

[39] MAVRIKAKIS M, HAMMER B N, NØRSKOV J K. Effect of strain on the reactivity of metal surfaces. *Physical Review B*, 1998, **81(13):** 2819.

[40] PANG Q, ZHANG Y, ZHANG J M, *et al.* Structural and electronic properties of atomic oxygen adsorption on Pt(111): a density-functional theory study. *Applied Surface Science*, 2011, **257(7):** 3047.

[41] KATTEL S, WANG G. Beneficial compressive strain for oxygen reduction reaction on Pt (111) surface. *Journal of Chemical Physics*, 2014, **141(12):** 124713.

[42] JACOBS R, HWANG J, SHAO-HORN Y, *et al.* Assessing

correlations of perovskite catalytic performance with electronic structure descriptors. *Chemistry of Materials*, 2019, **31(3):** 785.

[43] DEMAISON J, CSÁSZÁR A G. Equilibrium Co bond lengths. *Journal of Molecular Structure*, 2012, **1023:** 7.

弹性应变对 C、H、O 在过渡金属氧化物表面吸附的影响

谢 天[1], 宋二红[2]

(1. 上海交通大学 材料科学与工程学院, 上海 200240; 2. 中国科学院 上海硅酸盐研究所, 上海 200050)

摘 要: 目前铂(Pt)基贵金属催化剂(PGMs)是应用最广泛的商业催化剂, 但存在成本高、储量低、易引发小分子中毒的问题, 过渡金属氧化物(TMOs)因在氧化环境中具有较好的稳定性和出色的催化性能而被视为 PGMs 的潜在替代品。本研究通过密度泛函理论(DFT)计算, 全面分析了弹性应变对 TMOs 表面上碳(C)、氢(H)和氧(O)吸附能的影响。系统探究了这些影响在四方结构(PtO_2、PdO_2)和六方结构(ZnO、CdO)中的作用, 以及它们与各自过渡金属的关系。结果显示, 在金属氧化物表面上, 最有利的吸附位点主要位于氧原子顶部或金属原子顶部, 而过渡金属则更倾向于面心立方(FCC)和六方密排(HCP)的空位。此外, 在弹性应变的影响下, 虽然 TMOs 和过渡金属对 H 和 O 的吸附能存在很大差异, 但弹性应变对 TMOs 上 C、H 和 O 吸附能的影响与过渡金属类似: 在压缩应变下吸附能增加、吸附减弱, 而在拉伸应变下吸附能减小、吸附增强。这种现象可以用基于吸附发生在金属原子顶部时的 d 带模型或吸附发生在 O 原子顶部时的 p 带模型来合理解释。因此, 调控弹性应变也可用于改变 TMOs 的催化特性。

关 键 词: 密度泛函理论; 吸附能; 弹性应变工程; 过渡金属氧化物; 催化剂

中图分类号: TQ174 **文献标志码:** A **文章编号:** 1000-324X(2024)11-1292-09

Supporting Information:

Effect of Elastic Strains on Adsorption Energies of C, H and O on Transition Metal Oxides

XIE Tian[1], SONG Erhong[2]

(1. School of Materials Science and Engineering, Shanghai Jiao Tong University, Shanghai 200240, China; 2. Shanghai Institute of Ceramics, Chinese Academy of Sciences, Shanghai 200050, China)

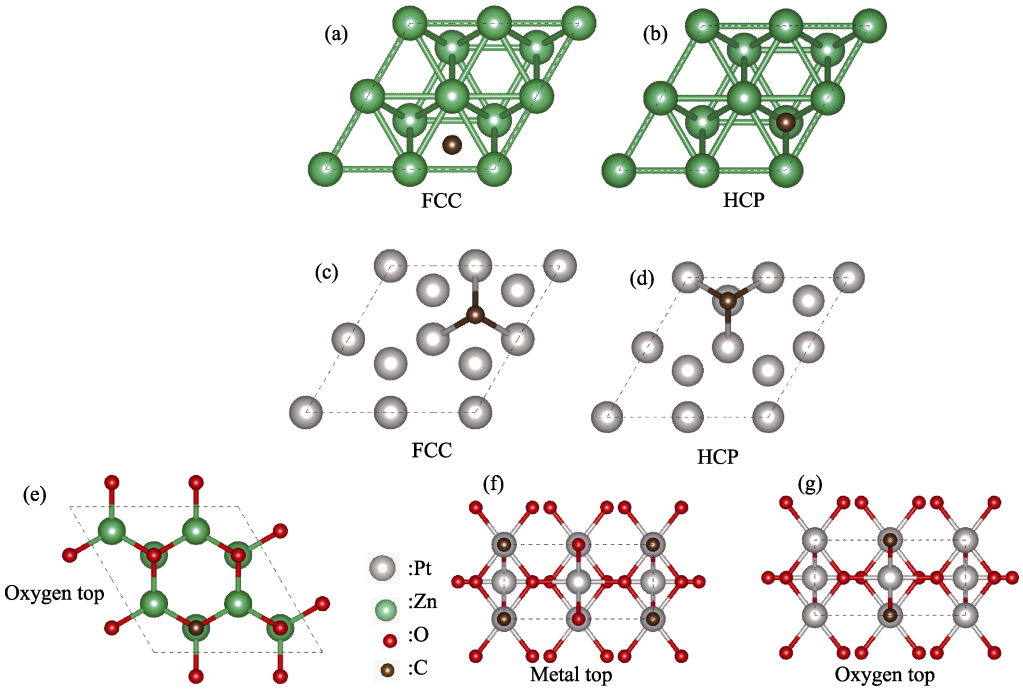

Fig. S1　Schematic diagram of the most stable adsorption site

(a, b) C adsorbed on Zn surface (a) FCC site and (b) HCP site; (c, d) C adsorbed on Pt surface (c) FCC site and (d) HCP site; (e) The most stable adsorption site for C atom on the ZnO surface; (f, g) C adsorbed on PtO_2 surface (f) metal top site and (g) oxygen top site

Colorful figures are available on website

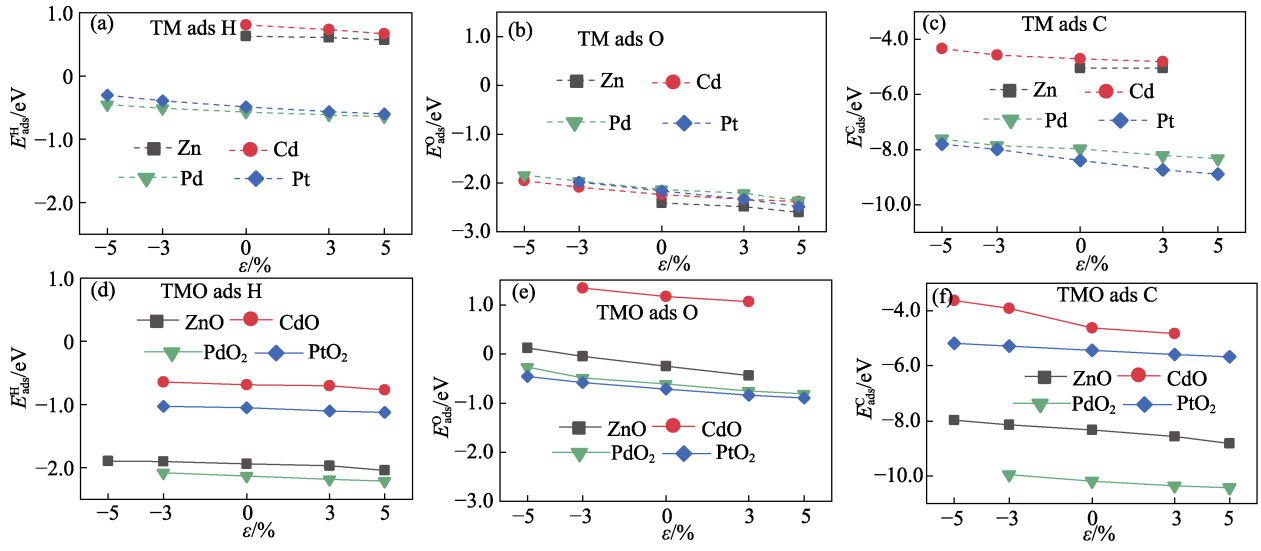

Fig. S2　Effect of biaxial elastic strains ε on adsorption energies of H, O and C on TM and TMO

(a) H on TM; (b) O on TM; (c) C on TM; (d) H on TMO; (e) O on TMO; (f) C on TMO

Table S1 Adsorption energy (eV) for H, O, and C on TM

Adsorbate	Zn			Cd			Pd			Pt		
	H	O	C	H	O	C	H	O	C	H	O	C
Top metal	0.88	–0.23	–4.33	1.13	–0.19	–2.88	–0.18	–0.77	–6.92	–0.11	–0.48	–6.36
Bridge	0.71	–1.55	–4.57	0.84	–1.69	–3.04	–0.41	–1.65	–7.13	–0.35	–1.76	–7.22
FCC	0.68	–2.26	–5.04	0.81	–2.24	–3.92	–0.57	–2.11	–7.97	–0.49	–2.16	–8.39
HCP	0.63	–2.41	–4.79	0.83	–2.21	–3.85	–0.48	–1.98	–7.63	–0.44	–2.14	–8.13

HCP and FCC indicate adsorption in the corresponding holes of the TM lattice (Fig. 1); The most favorable adsorption sites for each TM and adsorbate are marked in red

Table S2 Adsorption energy (eV) and preferred adsorption sites for H, O, and C on TMO

Adsorbate	ZnO			CdO			PdO_2			PtO_2		
	H	O	C	H	O	C	H	O	C	H	O	C
M top	1.37	1.91	–6.16	1.68	3.14	–1.12	–0.77	–0.43	–9.86	1.12	–0.72	–5.43
O top	–1.94	–0.25	–8.32	–0.69	1.17	–4.61	–2.13	0.99	–6.45	–1.05	1.03	–2.17
M–O Bridge	–0.13	–0.15	–7.16	1.63	2.17	–3.85	–1.02	0.36	–6.52	0.98	–0.32	–2.22
Hollow	–0.37	–0.22	–8.22	–0.64	1.51	–4.26	–1.35	0.03	–6.88	0.86	–0.66	–2.85

HCP and FCC indicate adsorption in the corresponding holes of the TMO lattice, while M top and O top indicate adsorption on top of metal and oxygen atoms, respectively (Fig. 1); The most favorable adsorption sites for each TMO and adsorbate are marked in red

Table S3 Bader charges for selected atoms in ZnO, CdO, PdO_2, and PtO_2

	ZnO	CdO	PdO_2	PtO_2		ZnO	CdO	PdO_2	PtO_2
Adsorbed O	0.02	–0.41	–0.36	–0.47	Adsorbed O	0.43	–0.07	0.49	0.56
Charge O	–0.47	–0.98	–0.57	–0.71	Charge O	–1.08	–1.07	–0.76	–0.76
Charge M	1.32	1.23	1.68	1.98	Charge M	1.26	1.15	1.62	1.81
Surface O average	–1.03	–1.04	–0.72	–0.83	Surface O average	–1.15	–1.10	–0.85	–0.92
Surface M average	1.26	1.22	1.66	1.93	Surface M average	1.24	1.13	1.50	1.61
E_{ads}^{O} / eV	–0.25	1.17	–0.43	–0.72	E_{ads}^{H} / eV	–1.94	–0.69	–2.13	–1.05

Adsorbed O (or H) refers to the Bader charge of the O (or H) that is adsorbed on the surface; Charge O is the Bader charge of the O atoms on the surface that are closer to the adsorbate; Charge M is the Bader charge for the metallic atom closer to the adsorbate; Surface O (or M) average represents the averaged Bader charge of all O (or metallic) atoms on the first layer